



Photocatalytic degradation of ammonia with titania nanoparticles under UV light irradiation

Seyedeh Fatemeh Hashemi¹ · Samad Sabbaghi^{2,3} · Rahmatallah Saboori³ · Bahman Zarenezhad¹

Received: 8 July 2021 / Accepted: 19 April 2022 / Published online: 11 May 2022
© The Author(s), under exclusive licence to Springer-Verlag GmbH Germany, part of Springer Nature 2022

Abstract

Ammonia is one of the major pollutants of water resources, posing a serious threat to human health and the environment. Titania nanoparticles were used to examine the photocatalytic degradation of ammonia from an aqueous solution in this study. Titania nanoparticles (NPs) were first synthesized via the sol–gel method, then characterized using XRD, FTIR, DLS, EDX, FE-SEM, and TEM analyses. Four effective parameters (pH, initial concentration of pollutant, catalyst dosage, and irradiation time) for photocatalytic degradation were explored using Design-Expert Software. The greatest photocatalytic activity of titania NPs was found in optimal conditions, according to the findings (97%). The optimum amounts of catalyst dosage, initial pollutant concentration, irradiation time, and pH were obtained at 0.3 g/l, 1500 mg/l, 120 min, and 12, respectively. Furthermore, studies revealed that pH was the most efficient variable in comparison with others and that increasing the pH value from 8 to 12 boosted ammonia removal from 40 to 97%. NPs showed high stability as the ammonia removal decreased from 96.96% to 65% after four cycles. Generally, this research has created a precedent for the development of morphology-dependent photocatalysts for the degradation of organic contaminants.

Keywords Ammonia · Degradation · Efficiency · NPs · Photocatalyst · Titania

Introduction

Although ammonia is one of the compounds that is employed in the production of some chemical materials like urea, fertilizer, fiber, plastic, explosives, paper, and rubber, it is a common contaminant of water resources which consists of nitrogen and nutrients that can accelerate the eutrophication and growth of algae in aquatic environments and eventually make some ecological issues (Reli et al. 2015; Shavisi et al. 2014a, b; Shibuya et al. 2013; Zendezhaban et al. 2013). The damage caused by the presence of ammonia in water sources is too vital and dangerous. Ammonia contamination of water

sources causes far too much harm and is far too hazardous. Ammonia depletes the oxygen in the water, lowers the disinfection efficiency of chlorine, endangers aquatic life, and causes respiratory and skin problems in people when present in high amounts (Lee et al. 2002; Shavisi et al. 2014a, b; Shavisi et al. 2016). Drinking water includes 1.5 mg/l of ammonia, according to the World Health Organization (WHO). As a result, this level is higher than the limit to which water's taste and smell can be altered.

In the last decade, water pollution has become a global issue in world environmental community researches (Shavisi et al. 2016). Therefore, wastewater treatments like degradation of ammonia from wastewater is an important subject from an environmental point of view (Shibuya et al. 2013). In order to decrease the concentration of ammonia in wastewater, different types of treatment technique including physical and chemical methods such as biological treatment, ion exchange, breakpoint chlorination, electrochemical process, chemical deposition, adsorption, membrane, and advanced oxidation processes are employed (Zendezhaban et al. 2013). The most impressive technique is biological nitrification/denitrification rather than the other techniques, but has some drawbacks such as needing large types of equipment and

Responsible Editor: Sami Rtimi

✉ Samad Sabbaghi
sabbaghi@shirazu.ac.ir; samad.sabbaghi@uwaterloo.ca

¹ Department of Chemical Engineering, Faculty of Chemical, Petroleum and Gas Engineering, Semnan University, Semnan, Iran

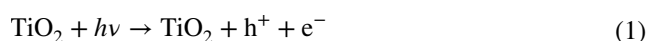
² Nanochemical Engineering Department, Faculty of Advanced Technologies, Shiraz University, Shiraz, Iran

³ Drilling Nano Fluid Lab, Shiraz University, Shiraz, Iran

having high operating costs. So, it makes secondary contamination and requires secondary purification for their degradation process completion (Lee et al. 2002; Reli et al. 2015). Chemical precipitation and adsorption techniques are frequently used to degrade low ammonia concentrations, but the drawbacks of chemical precipitation and adsorption methods might be secondary contamination and being limited by cation ions, respectively (Luo et al. 2015). The ion exchange procedure can eliminate ammonium ions from wastewater, but the secondary purification problem of ammonia is not gone away. In the breakpoint of the chlorination technique, by-products of converting aqueous ammonia to nitrogen and residual chlorine have to be treated again (Altomare et al. 2012).

According to the aforementioned disadvantages and drawbacks of techniques, the photocatalytic degradation method has been introduced as an alternative procedure of pollutant removal due to low energy consumption, low operating cost, simple operation, minimum secondary waste generation, and high efficiency (Shavisi et al. 2016; Zendezhaban et al. 2013). In photocatalytic reactions, choosing the right photocatalyst is very important (Shafiq et al. 2021a, b, c, d). Semiconductor compounds like titania NPs and zinc oxide NPs are employed to eliminate pollutants with the help of the photocatalytic technique. TiO_2 NPs have been widely employed as catalysts in the decontamination of aqueous solutions due to good stability, environmental compatibility, photochemical stability, low cost, non-toxicity, high efficiency, and oxidation ability of toxic substances (Altomare et al. 2012; Luo et al. 2015; Shavisi et al. 2014a, b).

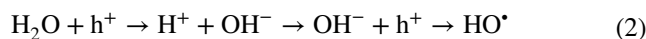
In semiconductor NPs, the electrons are stimulated by light irradiation and holes are created in the valence band, due to the existence of shifted electrons. The photocatalytic oxidation of titania NPs with light irradiation is as follows (Eq. 1) (Zhang et al. 2009):



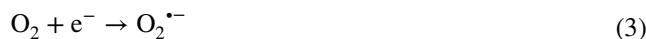
In photocatalytic reactions, there are both reduction and oxidation reactions. The oxidation reaction of H_2O and reduction reaction of O_2 are shown in Eqs. 2 and 3, 4, respectively (Shafiq et al. 2021a, b, c, d). The production of both reactions is OH radicals which can react with ammonia and generate less hazardous products (Shavisi et al. 2014a, b; Shafiq 2021). Oxidizing agents such as ozone, molecular oxygen, and tert-butyl hydroperoxide have been used in photocatalytic reactions (Shafiq et al. 2021a, b, c, d).

According to the previous studies, products of ammonia oxidation can be N_2 (Eqs. 6 and 8), NO_2^- , or NO_3^- (Eq. 8). Moreover, nitrite (NO_2^-) and nitrate (NO_3^-) can be reduced and produce N_2 which is a safe product (Liu et al. 2017; Luo et al. 2015) (Eqs. 10 and 11).

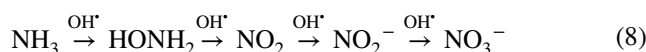
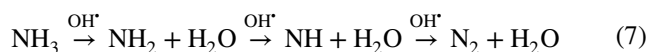
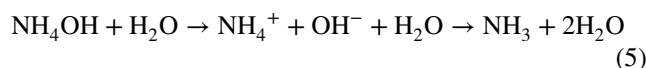
Photocatalytic oxidation:



Photocatalytic reduction:



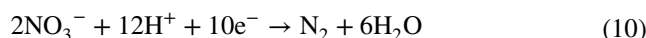
Ammonia reactions:



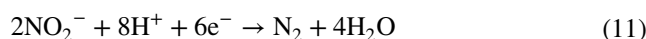
Oxidize ammonia:



Reduce nitrate:



Reduce nitrite:



The photocatalytic process is displayed in Fig. 1.

Owing to the decomposition of water, radicals are produced that oxidize ammonia pollutants (Eqs. 12 and 13) (Zendezhaban et al. 2013):



TiO_2 as a catalyst is used in too many chemical experiments. For instance, the performance of DBT under visible light was investigated by Kaveh Kalantari et al. (Shafiq 2021).

TiO_2 was employed as a photocatalyst in some research carried out by Toyoda et al. to eliminate dye. Toyoda et al. studied the removal of methylene blue (Toyoda et al. 2004). Li et al. investigated the degradation of methyl orange (MO), rhodamine B (Rho B), and methylene blue (MB) (Li et al. 2019). Mohammadi et al. eliminated methylene blue (Mohammadi et al. 2017), and in the other work, Malligavathy et al. evaluated the removal of Congo red dye (Malligavathy et al. 2016).

Recently, several scholars employed various metal oxides as a photocatalyst in photocatalytic degradation. The photocatalytic degradation of ammonia is studied by some researchers. Zendehzaban et al. investigated the photocatalytic removal of ammonia by TiO_2/Leca , and they found that by using this substance in the initial concentration of ammonia of 0.01 M and 30 g of photocatalyst and $\text{pH}=11$ and the duration of 300 min UV irradiation, more than 85% of ammonia contaminants have been removed (Zendehzaban et al. 2013). Sharifnia et al. studied the photocatalytic removal of ammonia from wastewater by using the zinc oxide particles stabilized on the Leca base (ZnO/Leca). The results of their experiments have shown that within 150 min of UV light, 57% of ammonia was removed (Sharifnia et al. 2013). Mohammadi et al. investigated the removal of ammonia by a photocatalyst TiO_2/ZnO immobilized on the Leca base ($\text{TiO}_2/\text{Leca ZnO}$). It has been observed that in $\text{pH}=11$, the initial concentration of 400 mg/l, contact time of 3 h, and catalyst dose of 25 g/l under UV irradiation equal to 92.5% have been achieved (Mohammadi et al. 2016). In another work, Shavisi et. al used TiO_2/l for the removal of ammonia (Shavisi et al. 2014a, b). Their experimental tests could be compared with the ones in this study. In that work (Shavisi et. al), the initial concentration of ammonia is 170 mg/l while in this work, the initial concentration of ammonia is much higher (1500 mg/l); the amount of catalyst is 11.7 g while the amount of catalyst in this study is 0.3 g/l; and ammonia removal is 68% after a 3-h UV irradiation time while in this study a dramatical removal equal to 96.96% is achieved. The results of these studies are presented in “Results and discussion” (Table 5). In this study, their tests are expanded by the changes in the amount of some parameters.

There are some studies that are focused on photocatalytic ammonia removal. In this study, there are several differences compared with the other studies. Design-Expert

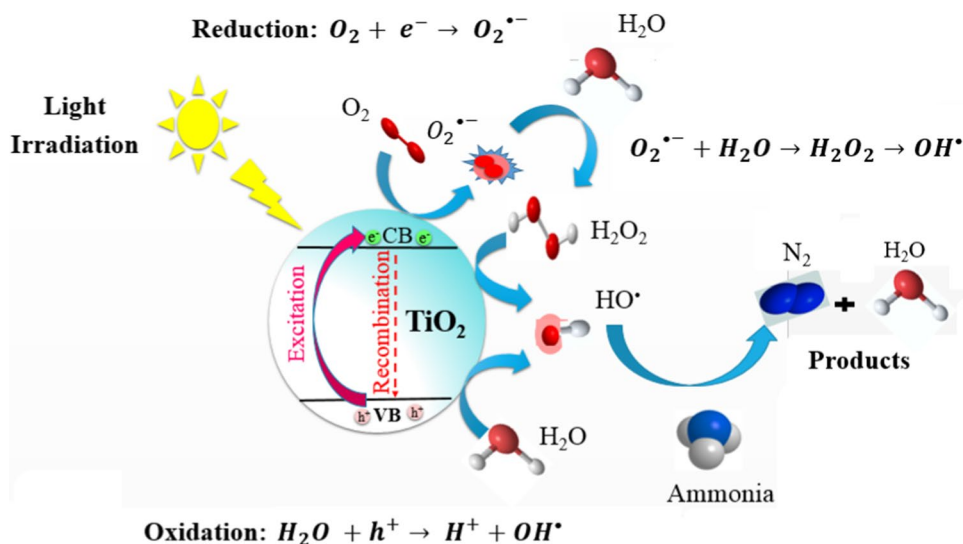
software is used for finding the various parameters’ effect on the optimum removal of ammonia and reducing the number of experiments while other studies did not use it. This study is carried out in a very high range of concentrations of ammonia (250–1500 mg/l), and in the highest concentration (1500 mg/l), ammonia removal is dramatically significant compared with other studies. The optimum amount of catalyst dose is 0.3 g/l (synthesized titania Nps) which is very slight. The reuse ability of Nps has been investigated. After four times of use, the removal rate was 65% which indicated that the catalyst is economical to use. It is mentioned that the titania NPs were synthesized by the sol–gel method and characterized by XRD, FTIR, DLS, EDX, FE-SEM, and TEM analyses. The effect of various parameters such as pH, ammonia concentration, catalyst dosage, and contact time, the intensity of UV and visible light irradiation, and aeration was investigated on the ammonia elimination, and the parameters were optimized.

Materials and method

Materials

Products tetraisopropoxide ($\text{Ti}(\text{OCH}(\text{CH}_3)_2)_4$, TTIP), nitric acid (HNO_3 , 65%), ethanol ($\text{C}_2\text{H}_5\text{OH}$, 99.9%), ammonium hydroxide (NH_4OH , 25%), and hydrochloric acid (HCl , 37%) were provided from Merck company. Moreover, sodium hydroxide (NaOH) was purchased from the Sinochem company. Deionized water (DW) was manufactured by the Zolal company. Ammonia reagent was prepared by the Hach company (USA) (contains Nessler’s reagent, mineral stabilizer, and polyvinyl alcohol).

Fig. 1 The photocatalytic process



Synthesis of titania NPs

The sol–gel method was used for synthesizing the titania NPs: A mixture of TTIP (5 ml) and ethanol (20 ml) was produced using a vigorous magnetic stirrer after 20 min at ambient temperature. After that, the solution was mixed with dilute nitric acid for 5–10 min at ambient temperature, and allowed to form sol and gel. The gel was dried at ambient temperature. At the final step, the powder was calcinated in a reactor at 400 °C for 4 h (Morgani et al. 2017).

Characterization of NPs

The dried nano-powder was characterized by XRD, FTIR, DLS, EDX, FE-SEM, and TEM analyses. The crystal structure of the sample was characterized by using an X-ray diffractometer and systematic X'Pert Pro XRD ($\lambda = 0.178$ 90 nm) in the range of 400–4000 cm^{-1} with KBr as the reference sample. A PerkinElmer FTIR (model: spectrum RXI), a TESCAN FE-SEM (model: MIRA III), and a Philips TEM (model: EM 208S) were used to characterize the NPs.

FTIR analysis is employed for organic compounds, but the peak of some other compounds such as metal oxides (TiO_2 , ZnO, CuO, etc.) can also be seen in FTIR. Figure 2 shows an FTIR analysis of the prepared TiO_2 NPs. The broad band of 2500–3600 cm^{-1} (3445 cm^{-1}) and the peak at 1644 cm^{-1} belong to an O–H functional group due to the asymmetrical stretching vibration in H_2O molecules. The band of carbonate groups was in the range of 1400 to 1540 cm^{-1} (1516 cm^{-1}), which is due to the absorption of CO_2 from the atmosphere into the ethanol solution. In the range of 500–1000 cm^{-1} , the Ti–O and Ti–O–Ti bonds have appeared. The FTIR spectrum confirms the stretching vibration peak of Ti–O at 677 cm^{-1} (Morgani et al. 2017; Sidane et al. 2017).

Figure 3 demonstrates the XRD pattern of the TiO_2 NPs. The peaks of the anatase TiO_2 NPs are $2\theta = 25.5$, 37.5, 48, 53, 55, and 62. The planes of (101), (004), (200), (211), and (204) of the synthesized TiO_2 catalyst coincide with anatase TiO_2 standard JCPDS Card no. 21–1272 (Zhang et al. 2018; Sadeghalvand and Sabbaghi 2015). Some weak peaks of the rutile phase are also observed in Fig. 3 which presents peaks at $2\theta = 27$, 36, and 55 corresponding to (110), (101), and (211) planes in rutile TiO_2 , respectively (standard JCPDS Card no. 88–1175). According to the XRD patterns, there are mixture peaks of anatase and rutile in the synthesized titania NPs. The anatase phase is dramatically higher than the rutile phase which is better for photocatalytic reactions (Thamaphat et al. 2008).

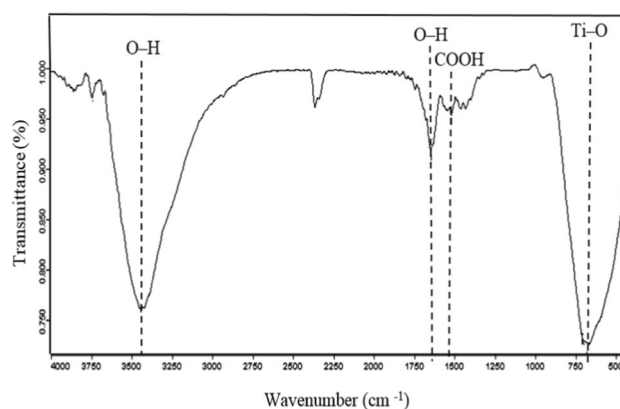


Fig. 2 FTIR pattern of the TiO_2 nanoparticles

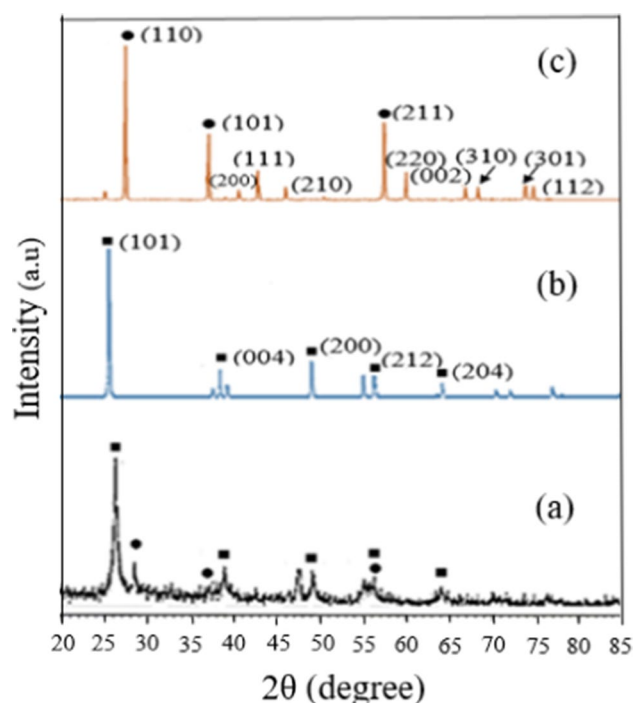


Fig. 3 XRD pattern of the TiO_2 nanoparticles

The average particle size of synthesized titania nanoparticles was determined using DLS analysis (Fig. 4). The particle size distribution of titania nanoparticles is narrow, with an average particle size of 60 nm, according to the findings.

The elemental composition of the TiO_2 NPs was determined using energy-dispersive X-ray spectroscopy (EDX, TESCAN VEGA 3). Figure 5 shows the EDX analysis of the TiO_2 nanoparticles. The EDX analysis revealed that these particles contain O and Ti elements. The peaks of the Ti and O elements and weight percentage of Ti and O atoms is shown in Fig. 5.

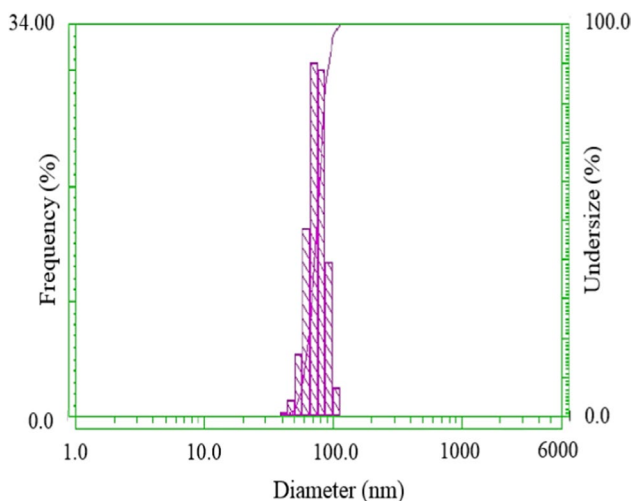


Fig. 4 Particle size distribution of TiO₂ nanoparticles

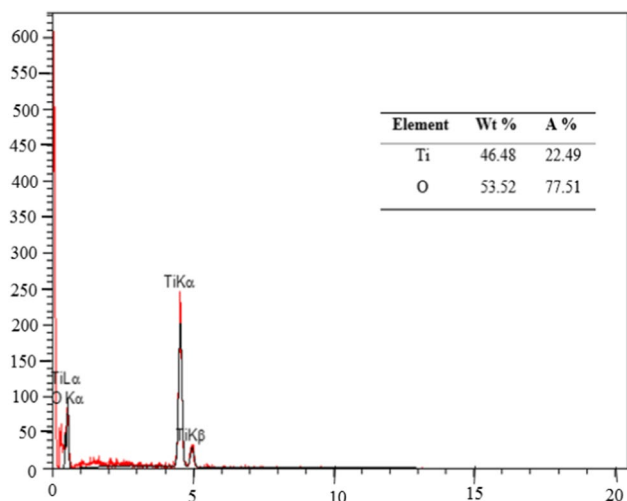
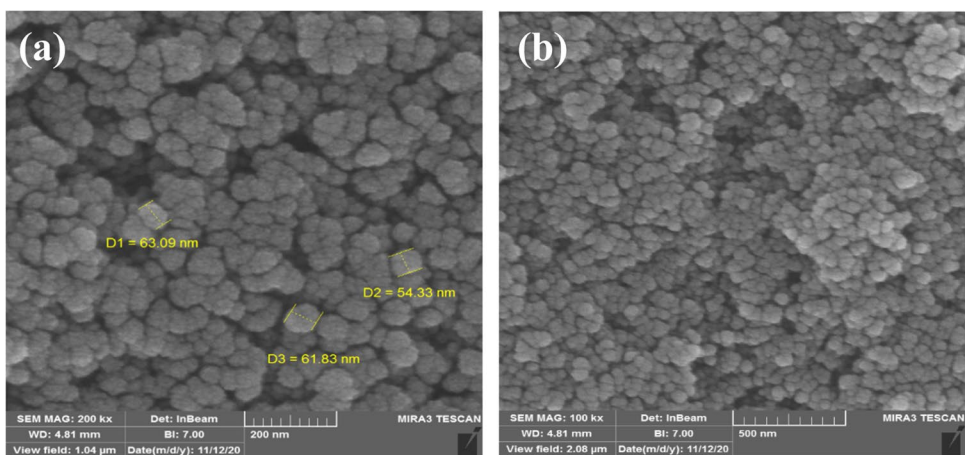


Fig. 5 EDX analysis of the TiO₂ nanoparticles

Fig. 6 FE-SEM image of the TiO₂ nanoparticles



The field emission scanning electron microscopy (FE-SEM) and (TEM) micrographs of TiO₂ NPs are shown in Figs. 6 and 7, respectively.

The size and morphology of TiO₂ NPs were analyzed by FE-SEM measurements. Figure 6a shows that the prepared TiO₂ has a spherical morphology, and the particle sizes of NPs are less than 60 nm. Figure 6b shows that the mean size of TiO₂ nanoparticles is about 60 nm.

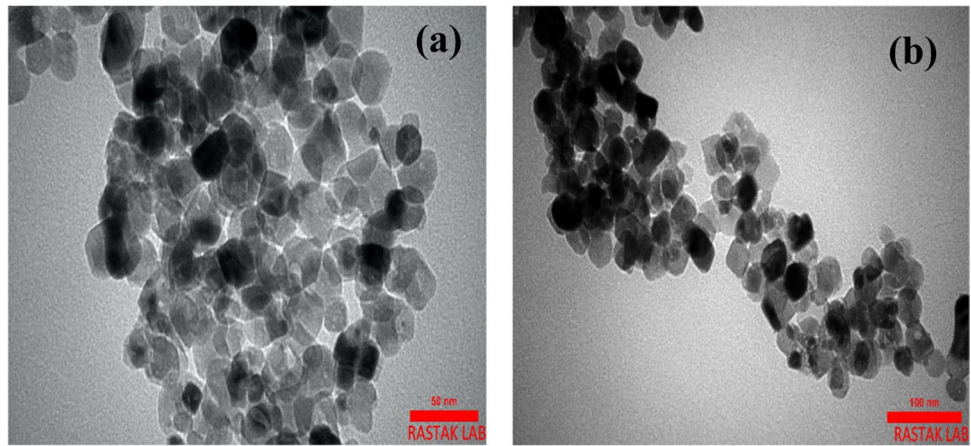
The TEM analysis was used for a better view of the TiO₂ NPs. The NPs have a spherical morphology with an average diameter about of 60 nm, which is in good agreement with the XRD and DLS analyses. TEM/EDX analyses confirmed the results obtained by XRD.

Investigation of the adsorption activity of TiO₂ NPs

The adsorption activity of nano-TiO₂ in the removal of ammonia from aqueous solution was investigated at the different ammonia concentrations, adsorbent concentration (nano-TiO₂ as an adsorbent), contact time, and pH. To determine the removal efficiency of ammonia, a specific amount of adsorbent was added to ammonia solution at a known pH and then was mixed at the known contact time at ambient conditions. After 120 min, 10 ml of sample was centrifuged. Eventually, the ammonia concentration was determined with UV–vis Spectrophotometer Jusco V-730 by adding Nessler’s reagent to the sample. The measured absorbance was at the wavelength of 425 nm which is considerable (Niedzielski et al. 2006). The removal percentage of ammonia was calculated by Eq. 14:

$$\text{Amminaremoval}(\%) = \frac{C_0 - C_t}{C_0} \times 100 \tag{14}$$

Fig. 7 TEM image of TiO₂



Based on the above equation, the ammonia concentration in solution is shown with C_0 and C_t (mg/L) at $t=0$ and at a contact time. The method of all experiments is based on the same system. Those were performed in a photocatalytic cylindrical reactor (Fig. 8). The light source is changed between two types, UV (T5, 8 W) and visible lamp (Xenon, 55 W) that is located in the center of the reactor, and the light is reflected in all directions. In the cooling chamber, water is used as a coolant and the temperature was kept at ambient temperature. An aeration pump was employed to create a uniform mixture (Shavisi et al. 2014a, b).

of ammonia elimination and also to reduce the number of experiments. The effective parameters for degrading ammonia consist of pH, initial concentration of ammonia, NP concentration, contact time, and type of light (UV and visible) (Mohammadifard et al. 2019). The number and the values of each level are presented in Table 1.

Results and discussion

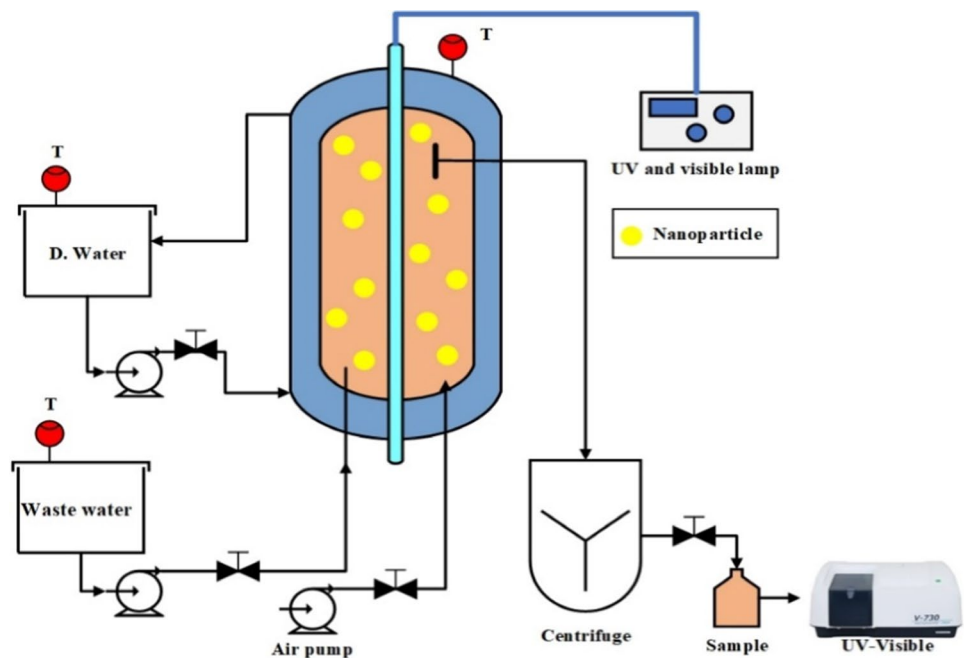
Designing the experiment and statistical investigations

Experimental design

Design-Expert software, version 10, Response Surface Methodology (RSM) (I-optimal), is used to find the effect of various parameters on the optimum condition

Design-Expert software suggested 19 some experiments with the different parameters' values. The experiments were designed, and the results for photocatalytic removal of ammonia are shown in Table 2. In statistical analysis of responses, the second-order polynomial equation is used

Fig. 8 Schematic of the reactor system



to predict responses based on the considered parameters (Eq. 15). The analysis of variance (ANOVA) was used to check the accuracy of the model. *F*-value (773.34), *P*-value (<0.0001), and *R*² (0.99) showed that the model has high accuracy. The amount of *P*-value for all parameters is shown in Table 3 and indicated that all parameters are effective in photocatalytic removal of ammonia (Niedzielski et al. 2006).

$$\begin{aligned} \text{Ammonia removal \%} = & +37.86 + (22.21 \times A) + (9.38 \times B) \\ & + (3.35 \times C) + (12.79 \times D) + (4.31 \times AD) \\ & + (6.22 \times B^2) - (6.66 \times C^2) + (6.06 \times D^2) \end{aligned} \tag{15}$$

Investigation of the effects of studied factors

The effect of initial ammonia concentration, pH, contact time, photocatalyst dosage, and contact time was investigated on the removal of ammonia by using analysis of variance (ANOVA).

The pH of a solution is the most effective parameter (based on the *F*-value) in the removal of ammonia by the photocatalytic method. The effect of pH on the removal of ammonia from the solution is shown in Fig. 9. It is obvious that the removal of ammonia enhances from 40% to about 97% with increasing pH value from 8 to 12. pH influences the surface charge nanoparticles and also the adsorption of ammonia on the photocatalyst surface and thus the rate of pollutant removal (Zhang et al. 2009).

According to the following Eqs. (16 and 17), in the presence of H⁺ (acidic ambient) and OH⁻ (alkaline ambient), the surface of TiO₂ can be protonated and deprotonated, respectively. Since the charge of ammonia is positive and

Table 1 Levels for each parameter

Name	Units	Levels							
		Levels	1	2	3	4	5	6	
Initial ammonia concentration	mg/l	6	250	500	750	1000	1250	1500	
Nano particle concentration	g/l	4	0.1	0.3	0.5	0.7	–	–	
pH	–	3	8	10	12	–	–	–	
Contact time	min	4	30	60	90	120	–	–	

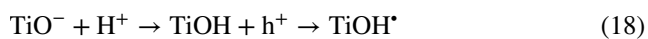
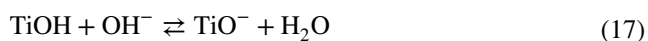
Table 2 Response surface methodology for photocatalytic removal of ammonia

Run	A: pH	B: Initial ammonia concentration (mg/l)	C: Nano particle concentration (g/l)	D: Contact time (min)	Removal (%)
1	8	250	0.3	30	8.84
2	8	1500	0.5	120	46.92
3	8	250	0.7	90	14.33
4	10	1000	0.1	30	24.76
5	12	250	0.7	120	76.93
6	12	1500	0.7	90	79.24
7	12	1500	0.3	120	97.25
8	12	1500	0.1	30	54.78
9	8	1500	0.1	60	18.58
10	10	1000	0.7	120	54.18
11	12	250	0.7	30	42.40
12	12	250	0.1	30	34.97
13	10	250	0.3	90	35.35
14	8	1500	0.7	30	24.40
15	12	750	0.3	90	63.38
16	10	250	0.3	90	38.74
17	8	250	0.1	120	16.98
18	8	1000	0.3	90	18.70
19	12	750	0.3	90	63.08

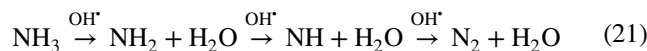
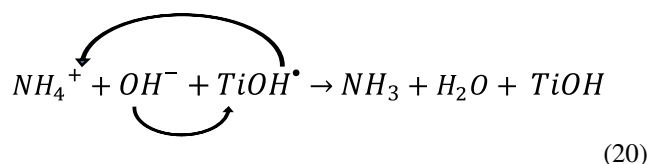
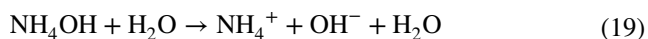
Table 3 Analysis of variance (ANOVA) photocatalytic removal of ammonia

	Sum of squares	df	Average of squares	F-value	P-value (probe > F)
Model	11,159.66	8	1394.96	773.34	0.0001 <
A: pH	7193.62	1	7193.62	3988.01	0.0001 <
B: Initial ammonia concentration	1166.94	1	1166.94	646.93	0.0001 <
C: Nanoparticle concentration	100.96	1	100.96	55.97	0.0001 <
D: Contact time	1533.46	1	1533.46	850.12	0.0001 <
AD	148.75	1	148.75	82.47	0.0001 <
B ²	117.50	1	117.50	65.14	0.0001 <
C ²	110.41	1	110.41	61.21	0.0001 <
D ²	112.30	1	112.30	62.26	0.0001 <

the surface of TiO₂ particles at alkali media get a negative charge and cationic types can be easily adsorbed, therefore photodegradation is done better at alkali conditions.



TiOH* is a source of hydroxyl radicals (•OH) to react with ammonia.



The point of zero charges (PZC) of TiO₂ NPs is about 6.3–6.8 (Shavisi et al. 2014a, b; Gong et al. 2015; Jamil and Sharaf El-Deen 2016). The point of zero charges is the pH at which the surface of the adsorbent is globally neutral. The zeta potential of TiO₂ NPs in the range of 4–12 is shown in Table 4 and Fig. 10. The relationship between zeta potential and the pH values is illustrated in Fig. 10. It is obvious that in pH=6.3, the zeta potential of the catalyst is zero (in the Smoluchowski model in pH=6.8, the zeta potential of the catalyst is zero). Below this value, the surface is positively charged; beyond this value, it is negatively charged. So normally, it is always easier to adsorb a cation on a negatively charged surface, and an anion on a positively charged surface (Zawawi et al. 2017). Therefore, at pH < pH_{zpc}, the surface charge of the catalyst is positive and at pH > pH_{zpc} it is negative (Shavisi et al. 2014a, b). According to Table 5, with

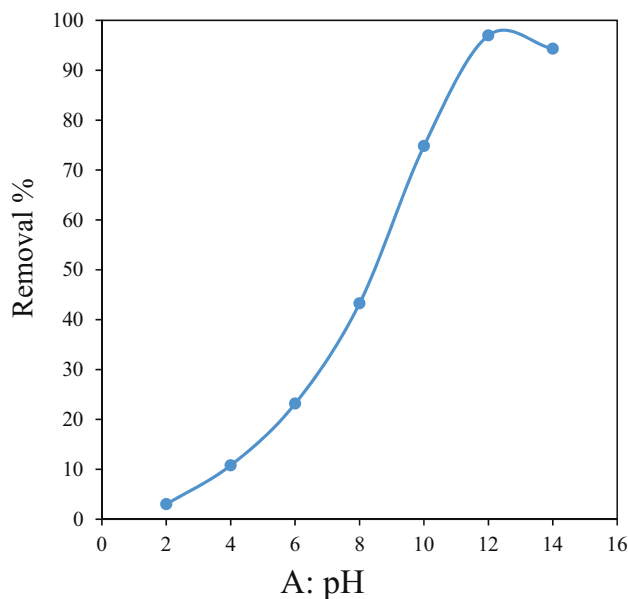


Fig. 9 Effect of pH on ammonia removal at initial ammonia concentration=1500 mg/l, nanoparticle concentration=0.3 g/l, and contact time=120 min

Table 4 Zeta potential values of the TiO₂

pH	Zeta potential (mv)
4	+40
5	+22
6.3	0
7	-10
8	-32.2
9	-40.5
10	-45.3
11	-49.7
12	-53.2

increasing pH, the surface of the catalyst has become more negative and the interaction between the catalyst surface with the available ammonium ions leads to strong absorption and eventually more pollutants are removed (Shavisi et al. 2014a, b). Also, with increasing pH, the number of hydroxyl ions (OH) gradually increased and as a result, more hydroxyl radicals ($\bullet\text{OH}$) are produced which increases the removal efficiency [8]. The ammonia interaction with the photocatalyst surface at pH = 12 was optimized and the ammonium ions are adsorbed at the highest surface. Under these conditions, the electron absorption by ammonium ions has resulted in a significant increase in the removal efficiency (Shavisi et al. 2016).

The effect of UV irradiation time on the photocatalytic removal of ammonia contaminant by using TiO_2 as photocatalyst is shown in Fig. 11. Experimental results showed that with the increase in contact time from 20 to 120 min, the removal rate increased from 60 to 96.96%. Residual ammonia decreased with UV irradiation time, and it is due to the fact that with the UV irradiation time increment, more hydroxyl radicals ($\bullet\text{OH}$) are produced which causes the performance of removal to enhance (Ghenaatgar et al. 2019). It is noteworthy that in all experiments, the reactor was placed in the dark for 30 min and then exposed to UV light irradiation for 120 min. The observed results are shown that the concentration of remaining ammonia in dark conditions was about 856 mg/l (42.87%). This amount of ammonia which was removed from the solution occurred via the adsorption process (Shavisi et al. 2014a, b). By using the titania photocatalyst, 96.96% of ammonia is removed from the solution after 120 min UV light irradiation (the maximum concentration of ammonia in the final solution was about 45 mg/l).

Another factor that influences ammonia removal is the initial concentration of ammonia. The effect of the initial concentration on the removal is shown in Fig. 12. Results showed that by increasing the initial concentration of ammonia, the removal efficiency increases due to the oxidation of OH^- anions and the generation of $\bullet\text{OH}$ radicals. In the concentration of more than 1000 (mg/l), the removal rate rapidly

enhances with increasing initial concentration, because the ammonia pollutant molecules can occupy all active sites of the photocatalyst (Mohsenzadeh et al. 2019).

An investigation was done on the evaluation of the effect of catalyst dose on the removal of ammonia, and results indicated that catalyst dose is a crucial factor in the photocatalytic removal of ammonia. In order to remove the ammonia, the effect of catalyst dose from 0.1 to 0.7 g/l was investigated. Figure 13 shows the effect of catalyst dose on the degradation efficiency. It is obvious that by increasing the catalyst dosage to 0.3 g/l, the number of active sites on the catalyst surface enhances, and this increase causes the interaction between the photocatalyst and the ammonia contaminant, and eventually, the removal rate enhances (Shavisi et al. 2014a, b). Also, the amount of absorbed photon increases and thus increases ammonia removal. Concentrations above 0.3 g/l may be due to inactivation of the active sites; with the decrease in the light intensity to the catalyst surface and limited hydroxyl radical ($\bullet\text{OH}$) production, the removal rate decreased (Song et al. 2013; Zhang et al. 2009). When the photocatalyst dosage is beyond its optimum amount, the solution becomes turbid and due to agglomeration of the photocatalyst as well as the lack of light penetrating deep into the solution, the efficiency of removal decreased (Dariani et al. 2016; Koe et al. 2020). Therefore, the optimum value of the catalyst dose is 0.3 g/l.

Investigation of the interactive effects of studied variables

One of the most advantages of RSM is that it studies the interaction between parameters and their effect on the removal of ammonia. Figure 14 shows the interaction between contact time and pH (AD) on ammonia removal. This figure shows that the removal rate of ammonia will increase with increasing contact time and pH. According to the analysis of variance (ANOVA) (Table 4), there is no

Fig. 10 Zeta potentials versus pH of the TiO_2 nanoparticles

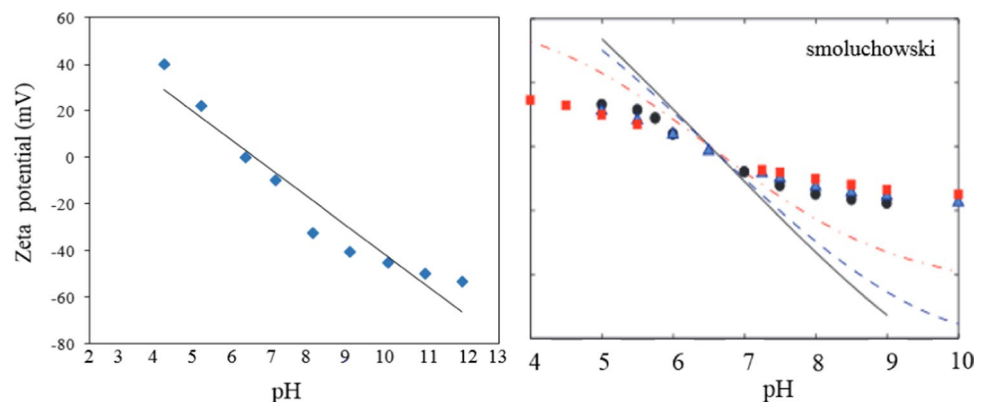


Table 5 Comparison of ammonia removal efficiency (%) using various photocatalysts

Photocatalyst	Removal conditions	Ref
TiO ₂ /perlite	Concentration: 170 mg/l Catalyst amount: 11.7 g Irradiation time: 3 h (UV light 125 W) Removal: 68%	Shavisi et al. (2014a, b)
SL g-C ₃ N ₄	Concentration: 1.5 mg/l Irradiation time: 6 h (UV light) Removal: 80%	Wang et al. (2014)
Pd/N/TiO ₂	Irradiation time: 2 h (visible light) Removal: 80%	Sun et al. (2015)
La/Fe/TiO ₂	Concentration: 100.67 mg/l Irradiation time: 5 h (UV light) Removal: 64.6%	Luo et al. (2015)
TiO ₂ -ZnO/LECA	Concentration: 400 mg/l Catalyst amount: 25 g/l Irradiation time: 3 h (visible light) Removal: 95.2%	Mohammadi et al. (2016)
Zn Fe ₂ O ₄ /rGO	Concentration: 100 mg/l Irradiation time: 4 h (visible light) Removal: 92.3%	Liu et al. (2017)
Cu/ZnO/rGO	Concentration: 50 mg/l Catalyst amount: 2 g Irradiation time: 2 h (visible light: Xe lamp) Removal: 83.2%	He et al. (2018)
Zn Fe ₂ O ₄ /AC	Concentration: 100 mg/l Catalyst amount: 25 g/l Irradiation time: 3 h (UV-visible light) Removal: 90%	Ye et al. (2019)
TiO ₂	Concentration: 1500 mg/l Catalyst amount: 0.3 g/l Irradiation time: 2 h (UV light) Removal: 96.96%	Present work

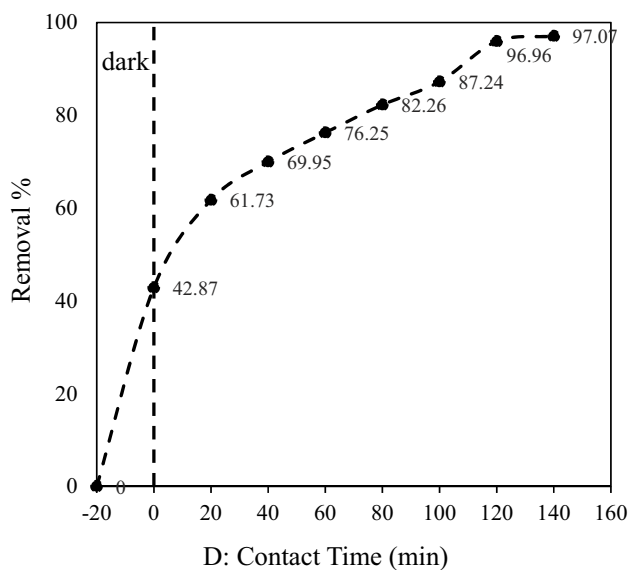


Fig. 11 Effect of contact time on removal of ammonia at pH=12, initial ammonia concentration=1500 mg/l, and nanoparticle concentration=0.3 g/l

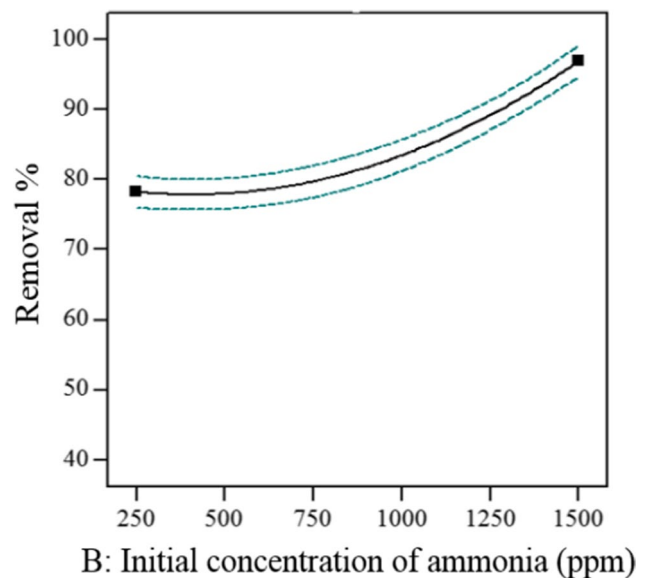


Fig. 12 Effect of initial concentration of ammonia on removal at pH=12, nanoparticle concentration=0.3 g/l, and contact time=120 min

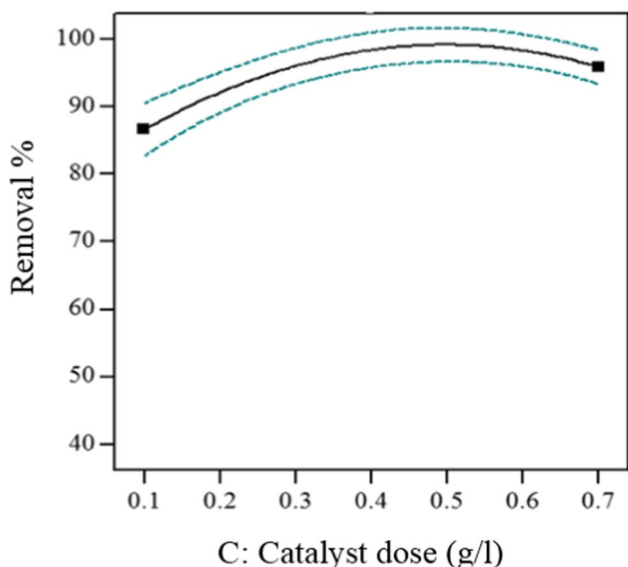


Fig. 13 Effect of catalyst dose on removal of ammonia at pH=12, initial ammonia concentration=1500 mg/l, and contact time=120 min

interaction between pH and ammonia concentration, so they can be regarded as independent parameters.

Optimum condition of ammonia removal

To investigate, the optimum condition for ammonia removal, initial concentration of ammonia, nanoparticle concentration, contact time, and pH were considered in the specific

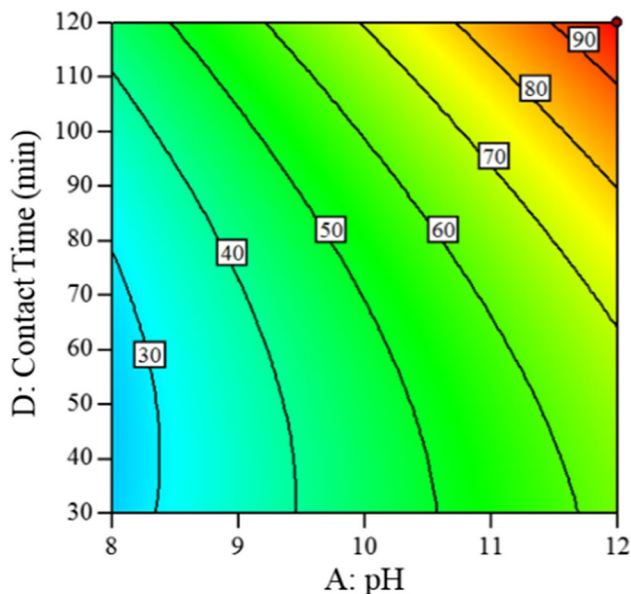


Fig. 14 Effect of interaction between pH and contact time on ammonia removal

ranges (Table 1). The initial concentration of ammonia was 1500 mg/l, and the removal rate was set to maximum. The results of ammonia removal in the optimum condition shown in Fig. 15. At the optimum condition, the highest ammonia removal was 96.96% and the highest desirability was 1.000. This optimum condition was repeated three times in the laboratory, and the removal efficiency was about 95.94%.

Effects of UV and visible light irradiation

Figure 16 shows the effect of two types of UV and visible light on the photocatalytic removal of ammonia by the TiO₂ photocatalyst. According to the outcomes, the optimum conditions (Fig. 15) under UV and visible light irradiation removal rates were 96.96% and 90.18%, respectively. This indicates that the rate of ammonia removal in the presence of UV light is higher than under the visible light, which is mainly due to the catalytic band gap. The band gap of photocatalyst is 3.2 eV showing that the UV light performs better than the visible light and the lower the band gap the performance is better in the presence of the visible light (Anandan et al. 2010). Figure 17(a) shows the UV–Vis diffuse reflectance spectra of calcined TiO₂ at 400 °C for 4 h. The synthesized photocatalyst absorbed light at a wavelength of 369 nm. As can be seen, the TiO₂ absorbance level increases at first and gradually decreases. In addition, according to the UV–Vis analysis and Eqs. 22 and 23, the TiO₂ Tauc plot is provided in Fig. 17(b).

$$E(h\nu) = \frac{hc}{\lambda} = \frac{1239.95}{\lambda} \tag{22}$$

$$\alpha = 2.303 \times d \tag{23}$$

$$(\alpha h\nu)^{\frac{1}{n}} = A(h\nu - E_g) \tag{24}$$

In Fig. 17(a), wavelength and absorbance are shown in horizontal and vertical parts, respectively. In Eq. 22, the band gap energy is shown by E (eV). In addition, h , c , and λ are Planck’s constant, the light velocity (m/s), and the light wavelength (nm), respectively (Hussain et al. 2010, 2011). In Eq. 23, the absorption coefficient and absorbance are shown by α and d , respectively. In Eq. 24, A is a proportionality constant and the amount of n for direct and indirect transition equals 1/2 and 2, respectively. Figure 17(b) shows the Tauc plot of TiO₂ nanoparticles. This figure (Fig. 17(b)) is plotted $(\alpha h\nu)^2$ versus $h\nu$ (Wang et al. 2011; Viezbicke et al. 2015). In the photocatalytic process, a metal oxide is activated with UV light, visible light, or sunlight. According to the previous studies, a metal oxide that has a higher band-gap (E_g) that can absorb over a large region of UV light as compared to visible light which is because of large excitation binding energy. In many studies, a band gap of rutile and anatase phase is reported to be about 3.0 and 3.2 eV,

Fig. 15 Optimum condition for ammonia removal by TiO₂ nanoparticle. (a) pH=12. (b) Initial concentration of ammonia (ppm)=1500. (c) Catalyst dose (g/l)=0.3. (d) Contact time (min)=120. (e) Removal %=96.9691

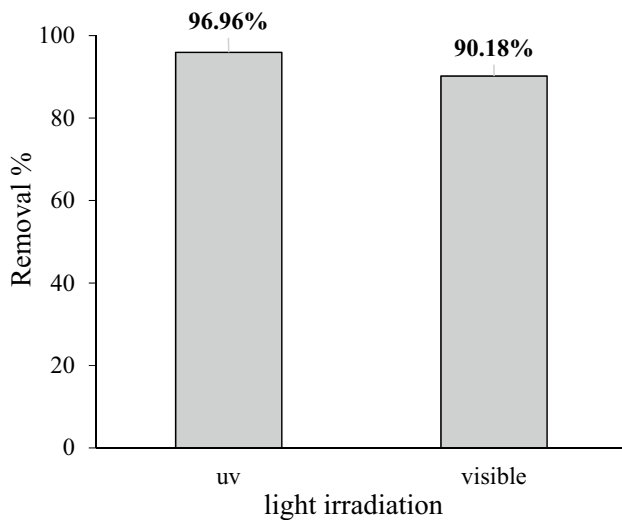
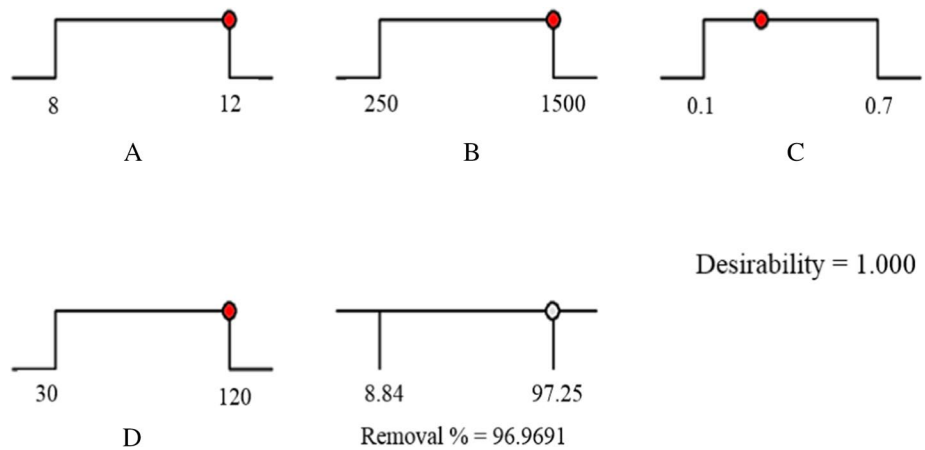


Fig. 16 Effect of two types of UV and visible light on removal of ammonia at pH=12, initial ammonia concentration=1500 mg/l, nanoparticle concentration=0.3 g/l, and contact time=120 min

respectively. The band gap of the synthesized photocatalyst is 3.2 eV, which shows that the anatase phase is dramatically higher than the rutile phase. The anatase phase has the highest photocatalytic activity because of an indirect band gap of the anatase phase (Phromma et al. 2020).

Effect of aeration

Figure 18 shows the effect of aeration on the photocatalytic removal of ammonia under optimum conditions (pH=12, catalyst dose=0.3 g/l, contact time=120 min, initial ammonia concentration=1500 mg/l, and UV-visible light).

The hydroxyl produced from the reduction of O₂ is shown in Eqs. 3 and 4 (Kolinko and Kozlov 2009). In the aeration condition and also in the absence of air, the removal efficiencies were about 96.96% and 89.86%. It is obvious that oxygen has not a strong effect on the photocatalytic removal of ammonia in an aqueous solution.

Fig. 17 UV-Vis DRS spectra for TiO₂ (a) and Tauc plot for band gap determination of TiO₂ nanoparticle (b)

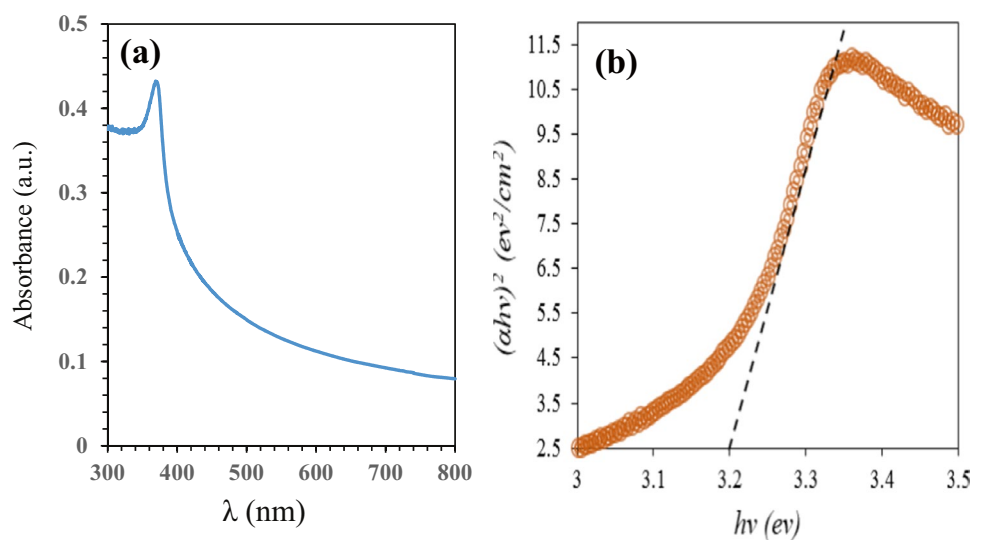
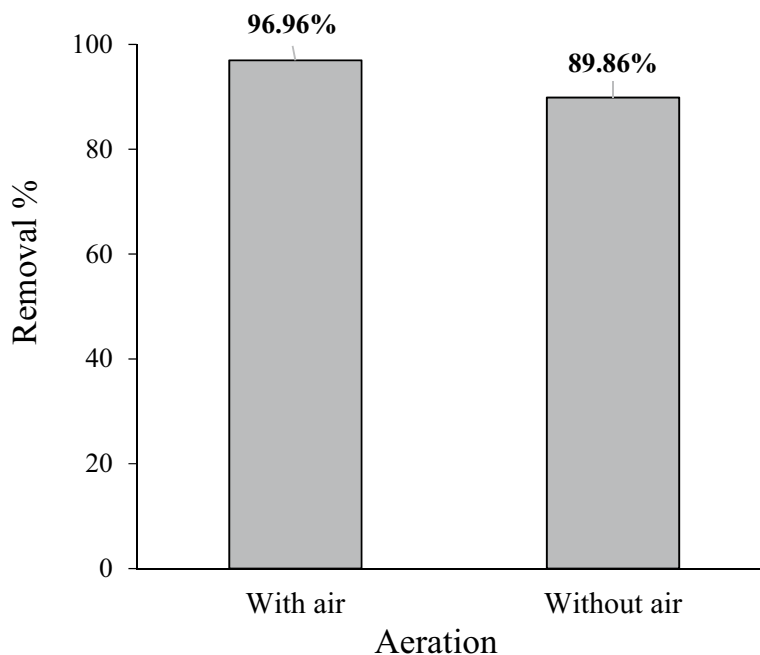


Fig. 18 Effect of aeration on removal of ammonia at pH=12, initial ammonia concentration = 1500 mg/l, nanoparticle concentration = 0.3 g/l and contact time = 120 min



Reusability of TiO_2 nanoparticles in the ammonia photocatalytic degradation process

The reusability of the photocatalyst is an important issue and has therefore been considered an essential issue. By using photocatalyst for a long time, its activity decreases, and ammonia molecules may block out some active sites which cover the surface of photocatalyst (Khan et al. 2015).

The reusability and stability of titania NPs at the initial ammonia concentration of 1500 mg/l, the NP concentration

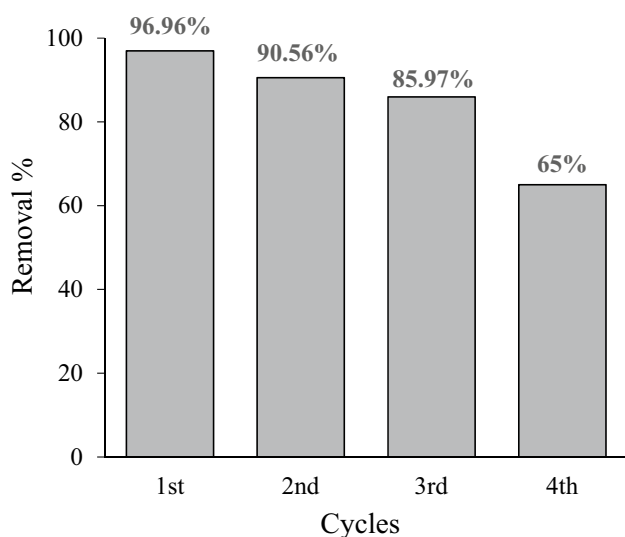


Fig. 19 Reusability of the TiO_2 nanoparticle for ammonia removal after each cycle in optimum condition

of 0.3 g/L, pH of 12, and contact time of 120 min are investigated. Centrifugation of the sample solution was carried out at 7000 rpm after 120 min of photocatalytic reaction, and the nanoparticles were separated. Then, the separated titania nanoparticles were reused for the next three times. Figure 19 shows the reusability of TiO_2 NPs for the removal of ammonia at the optimum condition. It is obvious that after four-times usage of the NPs, the rate of removal by the photocatalyst reduced and the removal rate decreased from 96.96% to 65% which indicates that the catalyst is economical to use.

Ammonia removal efficiency is compared with that in some previous study, and the removal condition is shown in Table 5. Results demonstrated that ammonia removes under UV or visible light with a higher catalyst amount and irradiation time. However, in the present work, TiO_2 removes 96.96% of ammonia using 0.3 g/l of the catalyst under a 2-h UV irradiation. To compare with other studies, the initial concentration of ammonia is much higher, and the amount of catalyst and irradiation time is lower than that in other studies; nevertheless, the removal efficiency is high.

Conclusion

The photocatalytic process has been regarded as a low-cost process for the purification of pollutants in water and wastewater. Also, the photocatalytic process is one of the most promising processes for efficient, economical, and environmentally friendly water and waste water treatment. The products are often less harmful, and environmentally friendly. In this study,

synthesizing the titania nanoparticles was carried out by the sol–gel method, and the NPs were characterized by the XRD, FTIR, DLS, EDX, FE-SEM, and TEM analyses. The photocatalytic performance of synthesized titania NPs on ammonia removal under UV light was studied by Design-Expert software (using the I-Optimal method). Also, the effect of factors such as NP concentration, contact time, pH, and initial ammonia concentration on the removal of ammonia from solution was investigated and determined the optimum conditions. According to the results, when it comes to the removal of ammonia by titania, pH is the most effective parameter. The removal rate increased with increasing pH from 8 to 12 and the highest removal rate was obtained at pH = 12. By increasing the catalyst dosage from 0.1 to 0.3 g/l, the removal rate augmented, and the highest efficiency of removal was achieved in the catalyst concentration of 0.3 g/l. The removal rate increased as a result of the contact time enhancement from 30 to 120 min, and initial ammonia concentration from 250 to 1500 mg/l. After 120 min, the removal rate was fixed. A reduction occurred in the removal efficiency of 96.96 to 65% after four times of reuse.

Author contribution Samad Sabbaghi: ideation, conceptualization, resources, supervision, project administration; funding acquisition, methodology.

SeyedehFatemeh Hashemi: conceptualization, methodology, software, formal analysis, investigation, writing (original and review), visualization.

Rahmatallah Saboori: Supervision, conceptualization, validation, visualization, methodology.

Bahman Zarenezhad: Resources, supervision, methodology, conceptualization.

All authors read and approved the final manuscript.

Data Availability The data that support the plots within this paper and other findings of the current study are available from the corresponding author upon reasonable request.

Declarations

Ethics approval and consent to participate Not applicable.

Consent for publication Not applicable.

Conflict of interest The authors declare no competing interests.

References

- Altomare M, Chiarello GL, Costa A, Guarino M, Selli E (2012) Photocatalytic abatement of ammonia in nitrogen-containing effluents. *Chem Eng J* 191:394–401. <https://doi.org/10.1016/j.cej.2012.03.037>
- Anandan S, Ohashi N, Miyauchi M (2010) ZnO-based visible-light photocatalyst: band-gap engineering and multi-electron reduction by co-catalyst. *Appl Catal B* 100(3–4):502–509. <https://doi.org/10.1016/j.apcatb.2010.08.029>
- Dariani RS, Esmaeili A, Mortezaali A, Dehghanpour S (2016) Photocatalytic reaction and degradation of methylene blue on TiO₂ nano-sized particles. *Optik* 127(18):7143–7154. <https://doi.org/10.1016/j.ijleo.2016.04.026>
- Ghenaatgar A, Tehrani RM, Khadir A (2019) Photocatalytic degradation and mineralization of dexamethasone using WO₃ and ZrO₂ nanoparticles: optimization of operational parameters and kinetic studies. *J Water Process Eng* 32:100969. <https://doi.org/10.1016/j.jwpe.2019.100969>
- Gong X, Wang H, Yang C, Li Q, Chen X, Hu J (2015) Photocatalytic degradation of high ammonia concentration wastewater by TiO₂. *Future Cities Environ* 1(1):1–12. <https://doi.org/10.1186/s40984-015-0012-9>
- He S, Hou P, Petropoulos E, Feng Y, Yu Y, Xue L, Yang L (2018) High efficient visible-light photocatalytic performance of Cu/ZnO/rGO nanocomposite for decomposing of aqueous ammonia and treatment of domestic wastewater. *Frontiers in Chem* 6:219. <https://doi.org/10.3389/fchem.2018.00219>
- Hussain M, Ceccarelli R, Marchisio DL, Fino D, Russo N, Geobaldo F (2010) Synthesis, characterization, and photocatalytic application of novel TiO₂ nanoparticles. *Chem Eng J* 157(1):45–51. <https://doi.org/10.1016/j.cej.2009.10.043>
- Hussain M, Russo N, Saracco G (2011) Photocatalytic abatement of VOCs by novel optimized TiO₂ nanoparticles. *Che Eng J* 166(1):138–149. <https://doi.org/10.1016/j.cej.2010.10.040>
- Jamil TS, Sharaf El-Deen SEA (2016) Removal of persistent tartrazine dye by photodegradation on TiO₂ nanoparticles enhanced by immobilized calcinated sewage sludge under visible light. <https://www.tandfonline.com/doi/abs/https://doi.org/10.1080/01496395.2016.1170036/>. Accessed 30 Mar 2016
- Khan MM, Adil SF, Al-Mayouf A (2015) Metal oxides as photocatalysts. *J Saudi Chem Society* 462–464
- Koe WS, Lee JW, Chong WC, Pang YL, Sim LC (2020) An overview of photocatalytic degradation: photocatalysts, mechanisms, and development of photocatalytic membrane. *Environ Sci Pollut Res* 27(3):2522–2565. <https://doi.org/10.1016/j.jscs.2015.04.003>
- Kolinko PA, Kozlov DV (2009) Products distribution during the gas phase photocatalytic oxidation of ammonia over the various titania based photocatalysts. *Appl Catal B* 90(1–2):126–131. <https://doi.org/10.1016/j.apcatb.2009.03.001>
- Lee J, Park H, Choi W (2002) Selective photocatalytic oxidation of NH₃ to N₂ on platinumized TiO₂ in water. *Environ Sci Technol* 36(24):5462–5468. <https://doi.org/10.1021/es025930s>
- Li Y, Wang W, Wang F, Di L, Yang S, Zhu S, Yu F (2019) Enhanced photocatalytic degradation of organic dyes via defect-rich TiO₂ prepared by dielectric barrier discharge plasma. *Nanomaterials* 9(5):720. <https://doi.org/10.3390/nano9050720>
- Liu SQ, Zhu XL, Zhou Y, Meng ZD, Chen ZG, Liu CB (2017) Smart photocatalytic removal of ammonia through molecular recognition of zinc ferrite/reduced graphene oxide hybrid catalyst under visible-light irradiation. *Catal Sci Technol* 7:3210–3219. <https://doi.org/10.1039/C7CY00797C>
- Luo X, Chen C, Yang J, Wang J, Yan Q, Shi H, Wang C (2015) Characterization of La/Fe/TiO₂ and its photocatalytic performance in ammonia nitrogen wastewater. *Int J Environ Res Public Health* 12(11):14626–14639. <https://doi.org/10.3390/ijerph121114626>
- Malligavathy M, Iyyapushpam S, Nishanthi ST, Padiyan DP (2016) Optimising the crystallinity of anatase TiO₂ nanospheres for the degradation of Congo red dye. *J Exp Nanosci* 11.13: 1074–1086. <https://doi.org/10.1080/17458080.2016.1186292>
- Mohammadi Z, Sharifnia S, Shavisi Y (2016) Photocatalytic degradation of aqueous ammonia by using TiO₂/ZnO/LECA hybrid photocatalyst. *Mater Chem Phys* 184:110–117. <https://doi.org/10.1016/j.matchemphys.2016.09.031>
- Mohammadi A, Aliakbarzadeh Karimi A (2017) Methylene blue removal using surface-modified TiO₂ nanoparticles: a comparative

- study on adsorption and photocatalytic degradation. *J Water Environ Sci Technol* 2(2):118–128. <https://doi.org/10.22090/jwent.2017.02.007>
- Mohammadifard Z, Saboori R, Mirbagheri NS, Sabbaghi S (2019) Heterogeneous photo-Fenton degradation of formaldehyde using MIL-100 (Fe) under visible light irradiation. *Environ Pollut* 251:783–791. <https://doi.org/10.1016/j.envpol.2019.04.143>
- Mohsenzadeh M, Mirbagheri SA, Sabbaghi S (2019) Degradation of 1, 2-dichloroethane by photocatalysis using immobilized Pani- TiO₂ nano-photocatalyst. *Environ Sci Pollut Res* 26(30):31328–31343. <https://doi.org/10.1007/s11356-019-06240-5>
- Morgani MS, Saboori R, Sabbaghi S (2017) Hydrogen sulfide removal in water-based drilling fluid by metal oxide nanoparticle and ZnO/TiO₂ nanocomposite. *Mater Res Express* 4(7):075501. <https://doi.org/10.1088/2053-1591/aa707b>
- Niedzielski P, Kurzyca I, Siepak J (2006) A new tool for inorganic nitrogen speciation study: simultaneous determination of ammonium ion, nitrite and nitrate by ion chromatography with post-column ammonium derivatization by Nessler reagent and diode-array detection in rain water samples. *Anal Chim Acta* 577(2):220–224. <https://doi.org/10.1016/j.aca.2006.06.057>
- Phomma S, Wutikhun T, Kasamechonchung P, Eksangsri T, Sapharoenkun C (2020) Effect of calcination temperature on photocatalytic activity of synthesized TiO₂ nanoparticles via wet ball milling sol-gel method. *Appl Sci* 10(3):993. <https://doi.org/10.3390/app10030993>
- Reli M, Ambrožová N, Šihor M, Matějová L, Čapek L, Obalová L, Kočí K (2015) Novel cerium doped titania catalysts for photocatalytic decomposition of ammonia. *Appl Catal B* 178:108–116. <https://doi.org/10.1016/j.apcatb.2014.10.021>
- Sadeghalvaad M, Sabbaghi S (2015) The effect of the TiO₂/polyacrylamide nanocomposite on water-based drilling fluid properties. *Powder Technol* 272:113–119. <https://doi.org/10.1016/j.powtec.2014.11.032>
- Shafiq I, Shafique S, Akhter P, Ishaq M, Yang W, Hussain M (2021b) Recent breakthroughs in deep aerobic oxidative desulfurization of petroleum refinery products. *J of Cleaner Production* 294:125731. <https://doi.org/10.1016/j.jclepro.2020.125731>
- Shafiq I, Hussain M, Rashid R, Shafique S, Akhter P, Yang W, Park YK (2021c) Development of hierarchically porous LaVO₄ for efficient visible-light-driven photocatalytic desulfurization of diesel. *Chem Eng J* 420:130529. <https://doi.org/10.1016/j.cej.2021.130529>
- Shafiq I, Hussain M, Shafique S, Akhter P, Ahmed A, Ashraf RS, Park YK (2021d) Systematic assessment of visible-light-driven microspherical V₂O₅ photocatalyst for the removal of hazardous organosulfur compounds from diesel. *Nanomaterials* 11(11):2908. <https://doi.org/10.3390/nano11112908>
- Shafiq I, Shafique S, Akhter P, Abbas G, Qurashi A, Hussain M (2021a) Efficient catalyst development for deep aerobic photocatalytic oxidative desulfurization: recent advances, confines, and outlooks. *Catal Reviews*: 1-46. <https://doi.org/10.1080/01614940.2020.1864859>
- Shavisi Y, Sharifnia S, Hosseini S, Khadivi M (2014a) Application of TiO₂/perlite photocatalysis for degradation of ammonia in wastewater. *J Ind Eng Chem* 20(1):278–283. <https://doi.org/10.1016/j.jiec.2013.03.037>
- Shavisi Y, Sharifnia S, Zendezhaban M, Mirghavami ML, Kakehazar S (2014b) Application of solar light for degradation of ammonia in petrochemical wastewater by a floating TiO₂/LECA photocatalyst. *J Ind Eng Chem* 20(5):2806–2813. <https://doi.org/10.1016/j.jiec.2013.11.011>
- Shavisi Y, Sharifnia S, Mohamadi Z (2016) Solar-light-harvesting degradation of aqueous ammonia by CuO/ZnO immobilized on pottery plate: linear kinetic modeling for adsorption and photocatalysis process. *J Environ Chem Eng* 4(3):2736–2744. <https://doi.org/10.1016/j.jece.2016.04.035>
- Shibuya S, Aoki S, Sekine Y, Mikami I (2013) Influence of oxygen addition on photocatalytic oxidation of aqueous ammonia over platinum-loaded TiO₂. *Appl Catal B* 138–139:294–298. <https://doi.org/10.1016/j.apcatb.2013.03.003>
- Sidane D, Khireddine H, Bir F, Yala S, Montagne A, Chicot D (2017) Hydroxyapatite-TiO₂-SiO₂-coated 316L stainless steel for biomedical application. *Metall Mater Trans A* 48(7):3570–3582. <https://doi.org/10.1007/s11661-017-4108-8>
- Song KS, Yu XC, Hu DD, Zheng X, Guo JY (2013) Photocatalytic degradation of ammonia nitrogen in aquaculture wastewater by using Nano-ZnO. *Adv Mat Res* 610(2013):564–568. <https://doi.org/10.4028/www.scientific.net/AMR.610-613.564>
- Sun D, Sun W, Yang W, Li Q, Shang JK (2015) Efficient photocatalytic removal of aqueous NH₄⁺-NH₃ by palladium-modified nitrogen-doped titanium oxide nanoparticles under visible light illumination, even in weak alkaline solutions. *Chem Eng J* 264:728–734. <https://doi.org/10.1016/j.cej.2014.12.012>
- Thamaphat K, Limsuwan P, Ngotawornchai B (2008) Phase characterization of TiO₂ powder by XRD and TEM. *Kasetsart J (Nat. Sci.)* 42.5: 357–361. <https://li01.tci-thaijo.org/index.php/anres/article/view/244620>
- Toyoda M, Nanbu Y, Nakazawa Y, Hirano M, Inagaki M (2004) Effect of crystallinity of anatase on photoactivity for methyleneblue decomposition in water. *Appl Catal B: Environ* 49(4):227–232. <https://doi.org/10.1016/j.apcatb.2003.12.012>
- Viezicke BD, Patel S, Davis BE, Birnie DP III (2015) Evaluation of the Tauc method for optical absorption edge determination: ZnO thin films as a model system. *Phys Status Solidi B* 252(8):1700–1710. <https://doi.org/10.1002/pssb.201552007>
- Wang D, Xiao L, Luo Q, Li X, An J, Duan Y (2011) Highly efficient visible light TiO₂ photocatalyst prepared by sol-gel method at temperatures lower than 300 °C. *J Haz Mat* 192(1):150–159. <https://doi.org/10.1016/j.jhazmat.2011.04.110>
- Wang H, Su Y, Zhao HX, Yu HT, Chen S, Zhang YB (2014) Photocatalytic oxidation of aqueous ammonia using atomic single layer graphitic-C₃N₄. *Environ Sci Technol* 48:11984–11990. <https://doi.org/10.1021/es503073z>
- Ye J, Liu SQ, Liu WX, Meng ZD, Luo L, Chen F, Zhou J (2019) Photocatalytic simultaneous removal of nitrite and ammonia via a zinc ferrite/activated carbon hybrid catalyst under UV-visible irradiation. *ACS Omega* 4(4):6411–6420. <https://doi.org/10.1021/acsomega.8b00677>
- Zawawi A, Ramli RM, Yub Harun N (2017) Photodegradation of 1-butyl-3-methylimidazolium chloride [Bmim] Cl via synergistic effect of adsorption-photodegradation of Fe-TiO₂/AC. *Technol* 5(4):82. <https://doi.org/10.3390/technologies5040082>
- Zendezhaban M, Sharifnia S, Hosseini SN (2013) Photocatalytic degradation of ammonia by light expanded clay aggregate (LECA)-coating of TiO₂ nanoparticles. *Korean J Chem Eng* 30(3):574–579. <https://doi.org/10.1007/s11814-012-0212-z>
- Zhang H, Wang X, Li N, Xia J, Meng Q, Ding J, Lu J (2018) Synthesis and characterization of TiO₂/graphene oxide nanocomposites for photoreduction of heavy metal ions in reverse osmosis concentrate. *RSC Adv* 8(60):34241–34251. <https://doi.org/10.1039/C8RA06681G>
- Zhang F, Feng C, Jin Y, Li W, Hao G, Cui J (2009) Photocatalytic degradation of ammonia nitrogen with suspended TiO₂. *Biomed Eng 3rd International Conference on pp* 1–4. <https://doi.org/10.1109/ICBBE.2009.5163185>

Publisher's note Springer Nature remains neutral with regard to jurisdictional claims in published maps and institutional affiliations.